Empirical formulas for particle production in P-Be collision between 10 and 35 BeV/c Part II

J. R. Sanford

May 1967

Collider Accelerator Department

Brookhaven National Laboratory

U.S. Department of Energy

DISCLAIMER

BROOKHAVEN NATIONAL LABORATORY JRS/CLW-2
Associated Universities, Inc.
Upton, L.I., N.Y.

ACCELERATOR DEPARTMENT
AGS
INTERNAL REPORT

EMPIRICAL FORMULAS FOR PARTICLE PRODUCTION IN

P-Be COLLISION BETWEEN 10 AND 35 BeV/c

(Part II)

J.R. Sanford and C.L. Wang

May 1, 1967

Part II - Kaon and Antiproton Production

1. General Form of the Empirical Formula

The empirical formula for pion productions presented in Part I of this

report proved to be successful both in representing the momentum spectra

and in predicting the pion multiplicities[1]. In view of the strong

resemblance in the general characteristics among the measured momentum

spectra of pion, kaon and antiproton productions[2,3], there is every

reason to believe that formulas of the same type as pion production

should apply equally well to kaon and antiproton productions.

The arguments for the angular dependence of the momentum spectra

and the forward production remain approximately valid, if not exactly.

On a semi-log plot one finds:

    1.   The ratio of the momentum spectra for θ degree production to

        zero degree production is well represented by a linear function.

        The slope of this linear function is independent of the incident

        proton momentum. Furthermore, the value of the linear function

exceeds unity at certain secondary momentum, say P_c. It is noticed that P_c is not zero but a decreasing function of θ and increasing function of the incident momentum.

2. For forward production, the momentum spectrum increases rapidly to a maximum and decays with a power greater than one as the secondary momentum increases from zero to its limit.

3. The kinematical constraint requires that the spectrum must vanish as the secondary momentum reaches the incident momentum.

4. Finally assuming the situation established in pion productions[1] is also true for kaons and antiprotons, we have that the transverse momentum distribution for kaon and antiproton productions is independent of the incident proton momentum which is greater than 10 BeV/c.

A formula for the double differential momentum spectrum that accommodates the above features reads:

$$\frac{d^2N}{d\Omega dp} = C_1 P^{C_2} (1 - \frac{P}{P_i}) e^{-\frac{C_3 P^{C_4}}{P_i^{C_5}}} - C_6 \theta (P - C_7 P_i \cos^{C_8} \theta)$$

where P and P_i are respectively the secondary and primary momenta in BeV/c, θ is the production angle in radian and C_1 through C_8 are unknown parameters to be determined by the least square analysis. For further details regarding the formula the reader is referred to Reference 1.

2. Least Square Analysis

The data employed in the analysis are from the same four experiments[2,3,4,5] which provided the pion production data. The importance of the relative normalization of the experimental data from various experiments with completely different experimental setup cannot be overemphasized, and was fully discussed and carefully explored in Reference 1. Accordingly, the absolute normalization was done relative to the data of Dekkers et al.[2],

and all data were converted into $(\frac{d^2N}{d\Omega dp})_k$ whose units are in number of

kaons/sr/BeV/c/interacting proton.

$$(\frac{d^2N}{d\Omega dp})_k = \frac{N_L}{\sigma_a} (\frac{d^2\sigma}{d\Omega dp})_k, \text{ Lundy et al.}$$

$$= \frac{1}{\sigma_a} (\frac{d^2\sigma}{d\Omega dp})_k, \text{ Dekkers et al.}$$

$$= \frac{1}{\eta} (\frac{d^2N}{d\Omega dp})_k, \text{ Fitch et al.}$$

$$= (\frac{d^2N}{d\Omega dp})_\pi \cdot R \text{ Baker et al.}$$

where σ_a (= 227 mb)[6] is the absorption cross section for P-Be collision,

N_L (= 1.5)[1] is the normalization factor for the data of Lundy et al[3].,

$(\frac{d^2N}{d\Omega dp})_\pi$ is the pion production calculated by means of the formulas of

Reference 1, η (= .6) is the internal target efficiency for the experiment

of Fitch et al[5] and

$$R = (\frac{d^2N}{d\Omega dp})_k / (\frac{d^2N}{d\Omega dp})_\pi$$

is the measured ratio of the intensities of kaon to pion productions. Values

of R from P-Al as well as P-Be collisions were used in the analysis as they

are consistent with each other within the experimental error. Relations

similar to equations (2) were used in the analysis of antiproton production.

The least square analyses were carried out by means of the FORTRAN

Program "LEAST"[7] at the computer CDC-6600 by minimizing the quantity

$$Q = \frac{1}{F} \sum_i \left[\frac{\log (\frac{d^2N}{d\Omega dp})^e_i - \log (\frac{d^2N}{d\Omega dp})^c}{\Delta (\frac{d^2N}{d\Omega dp})^e_i / (\frac{d^2N}{d\Omega dp})^e_i} \right]^2$$

where the superscript e and c refer to the experimental and calculated values

respectively, $\Delta (\frac{d^2N}{d\Omega dp})^e_i$ is the error pertaining to the i-th experimental

datum and F is the number of degrees of freedom in the least square fitting.

Good fits were obtained for $K^\pm$ and $\bar{p}$ respectively with the following

parameters.

	c_1	c_2	c_3	c_4	c_5	c_6	c_7	c_8	data	Q
K^+	.05897	.6916	3.744	4.520	4.190	4.928	.1922	50.28	72	0.58
K^-	.02210	1.323	9.671	1.712	1.643	4.673	.1686	77.27	54	1.40
$\bar{p}$	.001426	1.994	9.320	1.672	1.480	4.461	.2026	78.00	45	.42

The calculated momentum spectra together with the experimental data
were plotted by a CALCOMP plotter and are presented in Figure 1 through
Figure 24.

4.   Multiplicities, mean Secondary and Transverse Momenta, and Inelasticities.

The multiplicity M, mean secondary momentum <p>, mean transverse

momentum P_t and inelasticity I are defined respectively by

$$M = \int_0^{P_i} \int_0^{\pi} 2\pi \frac{d^2N}{d\Omega dp} \sin\theta d\theta dp$$

$$<p> = \frac{1}{N_\pi} \int_0^{P_i} \int_0^{\pi} 2\pi \frac{d^2N}{d\Omega dp} p \sin\theta d\theta dp$$

$$P_t = \frac{1}{N_\pi} \int_0^{P_i} \int_0^{\pi} 2\pi \frac{d^2N}{d\Omega dp} p \sin^2\theta d\theta dp$$

and

$$I = \frac{1}{P_i} \int_0^{P_i} \int_0^{\pi} 2\pi \frac{d^2N}{d\Omega dp} p \sin\theta d\theta$$

Unfortunately, there are no experimental measurements of these

quantities for kaon and antiprotons which may provide an independent check

to the validity of the empirical formulas. They are presented in the following

table for the sake of completeness and for future references. The integrations

were carried out numerically.

	P_i (BeV/c)	M	$\langle P \rangle$	P_t	I
K^+	10	.066	1.12	.255	.0074
	15	.085	1.54	.271	.0088
	20	.111	1.91	.284	.0106
	25	.145	2.21	.295	.0128
	30	.193	2.44	.304	.0157
	35	.260	2.61	.312	.0194
K^-	10	.012	1.09	.297	.0014
	15	.018	1.57	.312	.0019
	20	.026	2.05	.324	.0026
	25	.035	2.49	.334	.0035
	30	.046	2.90	.345	.0045
	35	.061	3.26	.355	.0057
$\bar{p}$	10	.0007	1.42	.342	.00010
	15	.0014	2.05	.354	.00019
	20	.0023	2.63	.365	.00031
	25	.0037	3.17	.378	.00047
	30	.0056	3.64	.393	.00068
	35	.0084	4.05	.408	.00097

5. Discussion

In pion productions, the experimental data at 13.4 and 18.8 BeV/c clearly demonstrate an interesting feature; namely, the low energy pions are more abundantly produced at certain angles rather than at zero degree. There is no evidence of this behavior for antiproton productions because of the non-existence of experimental data in the region of interest. However, for kaon production, there is an indication of this characteristic at 13.4 BeV/c incident momentum, although the quality of the data is relatively poor. At higher energies, again there is no experimental measurement.

It is therefore, very desirable to carry out a systematic experimental investigation of kaon and antiproton productions in the region of low secondary momentum (zero to about a quarter of the incident momentum). By systematic we mean, an experiment primarily designed to explore only those points which are crucial to the establishment of the characteristics of the kaon and antiproton production at low energy. The significance is two fold. Firstly, the study of the interesting characteristics mentioned above should contribute to the understanding of the production mechanisms

for which no adequate theory exists. This will at least establish better empirical formulas. Secondly, the study is directly benificial for practical application, because a substantial gain in the secondary beam flux can be obtained by choosing the correct angle of production for a given secondary momentum.

We appreciate the invaluable assistance of Miss Janet Head for the programming and the help of Mr. Fred Kuehl, Mr. Paul Hallowell and Mr. Malcolm McCrum in the data reduction.

<div align="center">References</div>

1. J.R. Sanford and C.L. Wang, Brookhaven National Laboratory, AGS Internal Report, 1967. (Unpublished).

2. D. Dekkers, J.A. Geibel, R. Mermod, G. Weber, T.R. Willitts, K. Winter, B. Jordan, M. Vivargent, N.M. King and E.J.N. Wilson, Physical Review, 137, B962 (1965).

3. R.A. Lundy, T.B. Novey, D.D. Yavanovitch and V.L. Telegdi, Physical Review Letters, 14, 504 (1966).

4. W.F. Baker, R.L. Cool, W.E. Jenkins, T.F. Kycia, S.J. Lindenbaum, W.A. Love, D. Luers, J.A. Niederer, S. Ozaki, A.L. Read, J.J. Russell and L.C.L. Yuan, Physical Review Letters 7, 101 (1961).

5. V.L. Fitch, S.L. Meyer and P.A. Pirone, Physical Review 126, 1849 (1962).

6. G. Belletlini, G. Cocconi, A.N. Diddens, E. Lillethan, G. Matthiae, J.P. Scanlon and A.M. Wetherall, CERN Report PS/5037/KL, (1965). (Unpublished).

7. F. Ragusa, "Modified Version of Los Alamos Code "PAKAG."" (In file at the BNL Program Library).

Fig. 1   Momentum spectra for K^+ production from P-Be collision at 10.9
          BeV/c incident momentum. The data are from Reference 4.

Fig. 2   Momentum spectra for K^+ production from P-Be collision at 13.4
          BeV/c incident momentum. The data are from Reference 3.

Fig. 3   Momentum spectra for K^+ production from P-Be collision at 18.8
          BeV/c incident momentum. The data are from Reference 2.

Fig. 4   Momentum spectra for K^+ production from P-Be collision at 20.9
          BeV/c incident momentum. The data are from Reference 4.

Fig. 5   Momentum spectra for K^+ production from P-Be collision at 23.1
          BeV/c incident momentum. The data are from Reference 2.

Fig. 6   Momentum spectra for K^+ production from P-Be collision at 27.0
          BeV/c incident momentum.

Fig. 7   Momentum spectra for K^+ production from P-Be collision at 30.9
          BeV/c incident momentum. The data are from Reference 4.

Fig. 8   Momentum spectra for K^+ production from P-Be collision at 33.9
          BeV/c incident momentum.

Fig. 9   Momentum spectra for K^- production from P-Be collision at 10.9
          BeV/c incident momentum. The data are from Reference 4.

Fig. 10   Momentum spectra for K^- production from P-Be collision at 13.4
          BeV/c incident momentum. The data are from Reference 3.

Fig. 11   Momentum spectra for K^- production from P-Be collision at 18.8
          BeV/c incident momentum. The data are from Reference 2.

Fig. 12   Momentum spectra for K^- production from P-Be collision at 20.9
          BeV/c incident momentum. The data are from Reference 4.

Fig. 13   Momentum spectra for K^- production from P-Be collision at 23.1
          BeV/c incident momentum. The data are from Reference 2.

Fig. 14   Momentum spectra for K^- production from P-Be collision at 27.0
          BeV/c incident momentum.

Fig. 15   Momentum spectra for K^- production from P-Be collision at 30.9
          BeV/c incident momentum. The data are from Reference 4.

Fig. 16   Momentum spectra for K^- production from P-Be collision at 33.9
          BeV/c incident momentum.

Fig. 17   Momentum spectra for $\bar{p}$ production from P-Be collision at 10.9
          BeV/c incident momentum.

Fig. 18   Momentum spectra for $\bar{p}$ production from P-Be collision at 13.4
          BeV/c incident momentum. The data are from Reference 3.

Fig. 19　Momentum spectra for $\bar{p}$ production from P-Be collision at 18.8 BeV/c incident momentum. The data are from Reference 2.

Fig. 20　Momentum spectra for $\bar{p}$ production from P-Be collision at 20.9 BeV/c incident momentum. The data are from Reference 4.

Fig. 21　Momentum spectra for $\bar{p}$ production from P-Be collision at 23.1 BeV/c incident momentum. The data are from Reference 2.

Fig. 22　Momentum spectra for $\bar{p}$ production from P-Be collision at 25.9 BeV/c incident momentum. The data are from Reference 4.

Fig. 23　Momentum spectra for $\bar{p}$ production from P-Be collision at 30.9 BeV/c incident momentum. The data are from Reference 4.

Fig. 24　Momentum spectra for $\bar{p}$ production from P-Be collision at 33.9 BeV/c incident momentum. The datum is from Reference 5.

10.9 BEV/C P-BE. POSITIVE KAON PRODUCTION
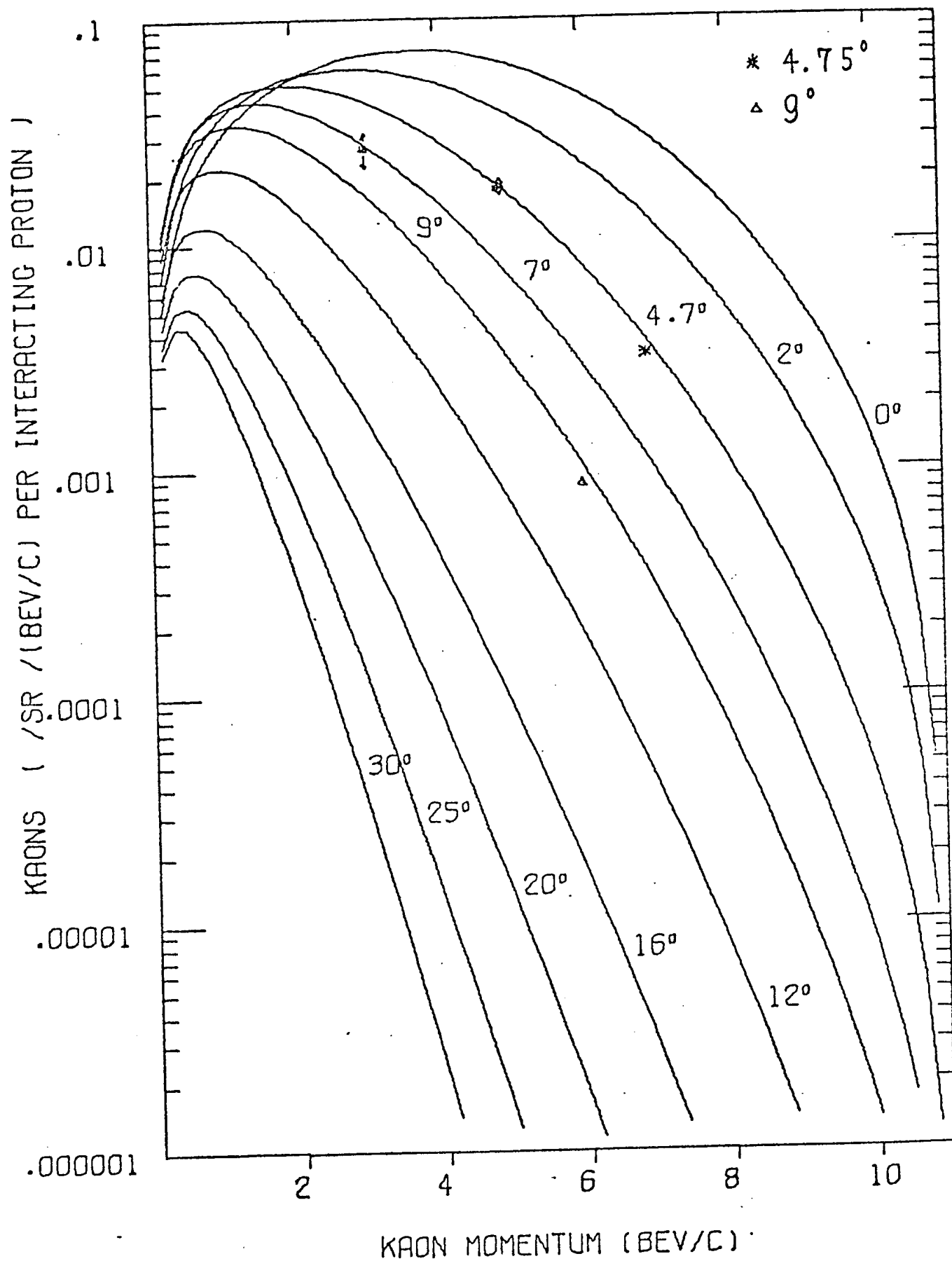
Figure 1

13.4 BEV/C   P-BE.   POSITIVE KAON PRODUCTION
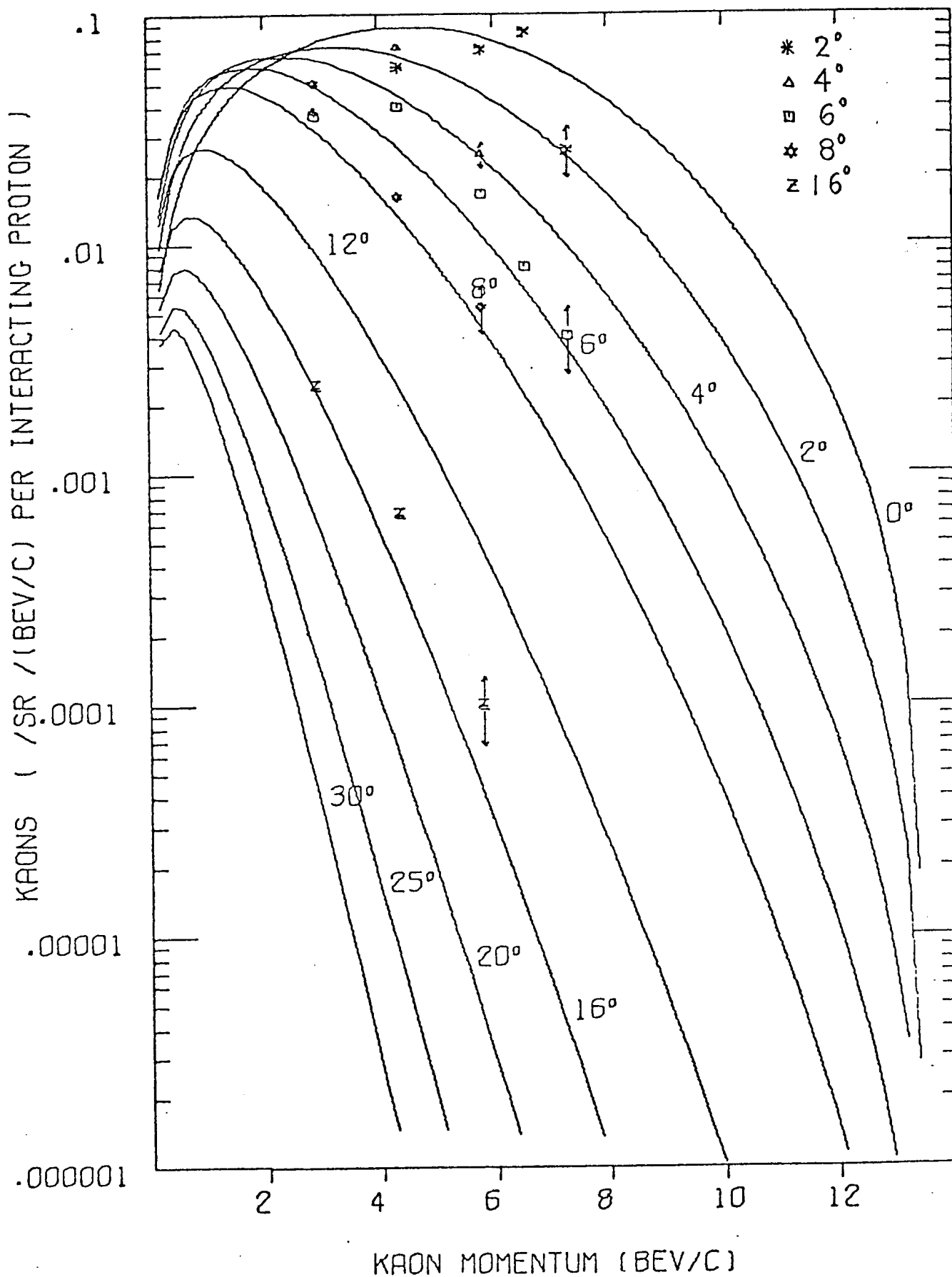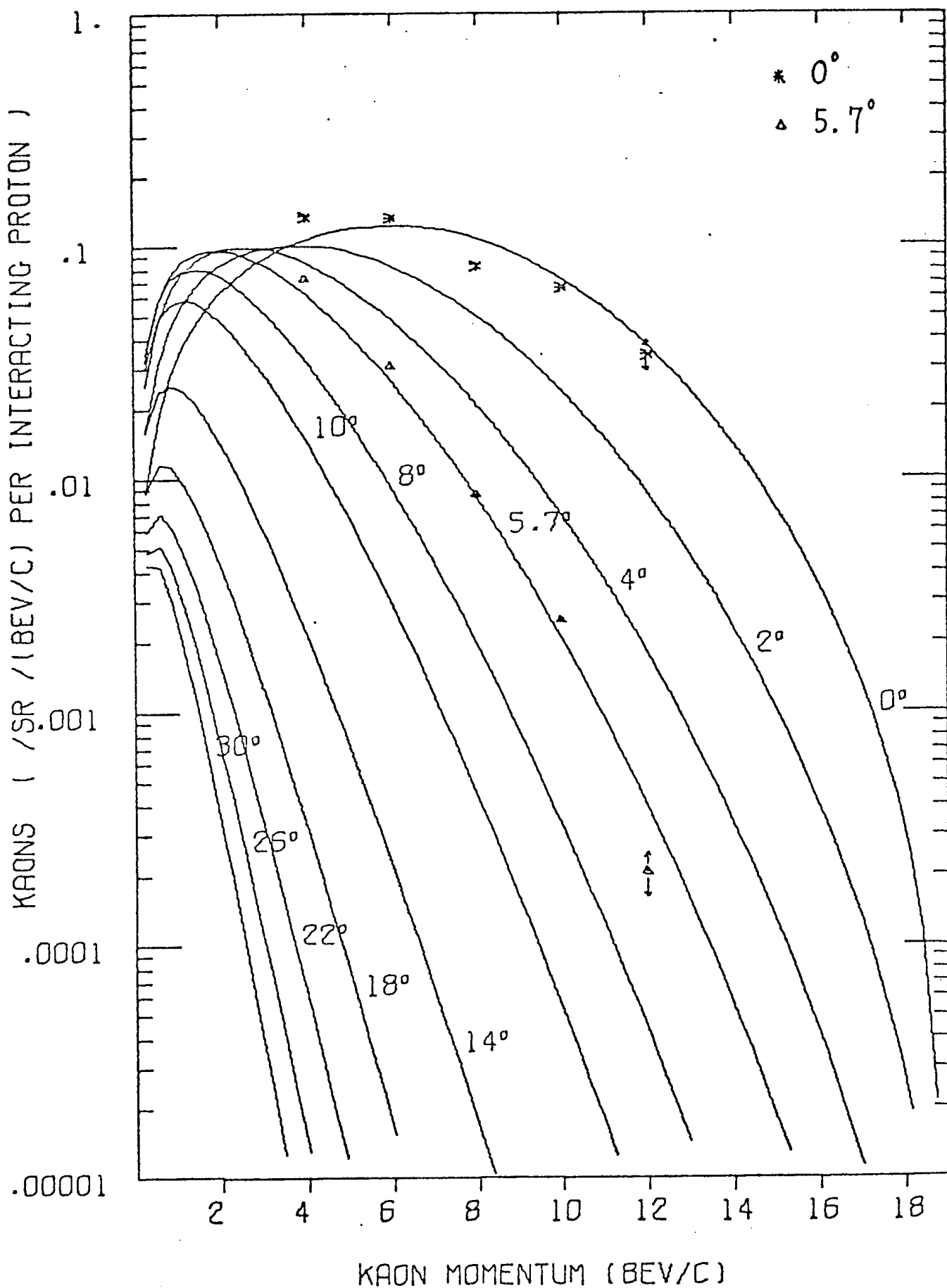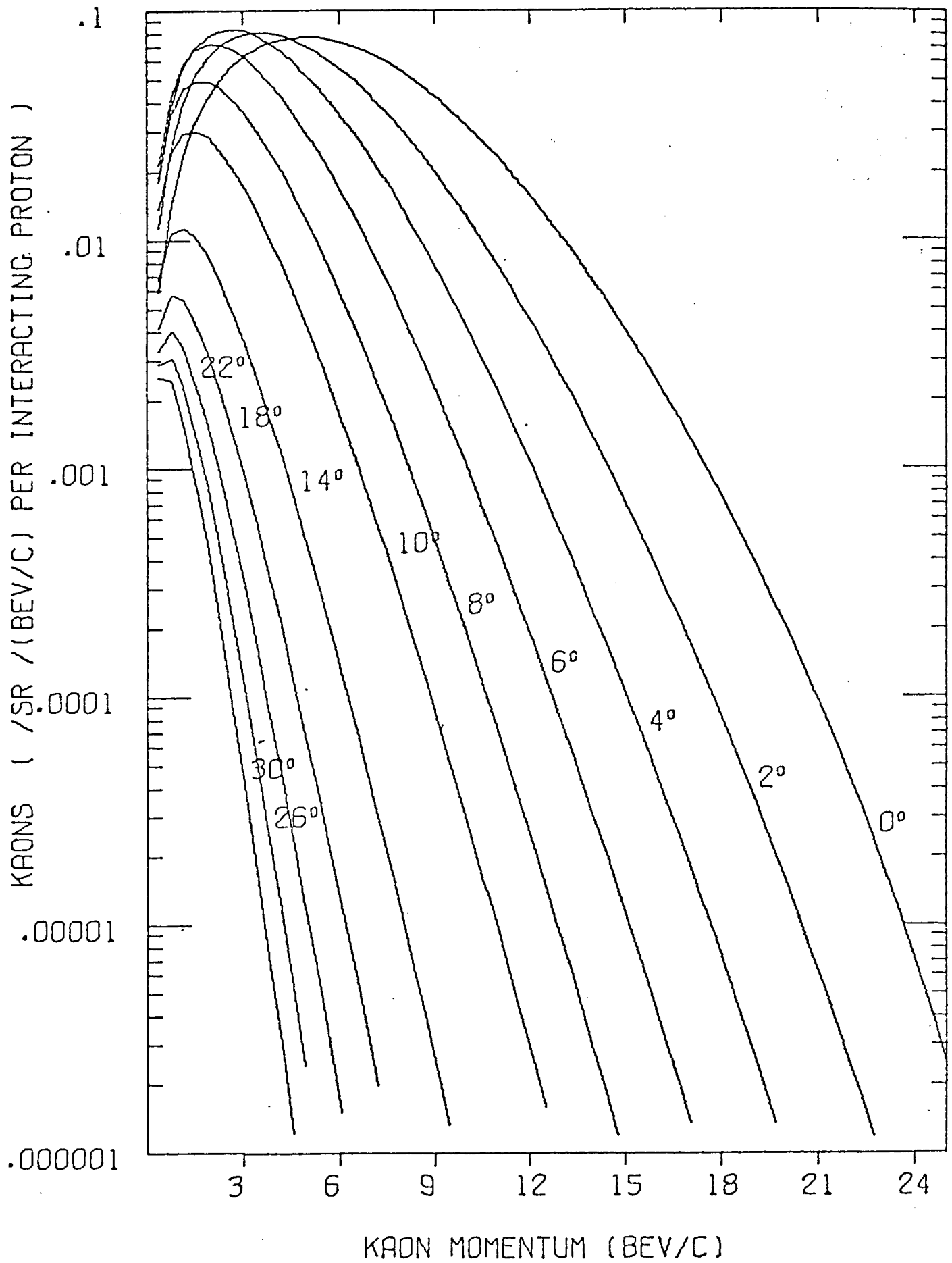

Figure 2

Figure 3

20.9 BEV/C   P-BE.   POSITIVE KAON PRODUCTION
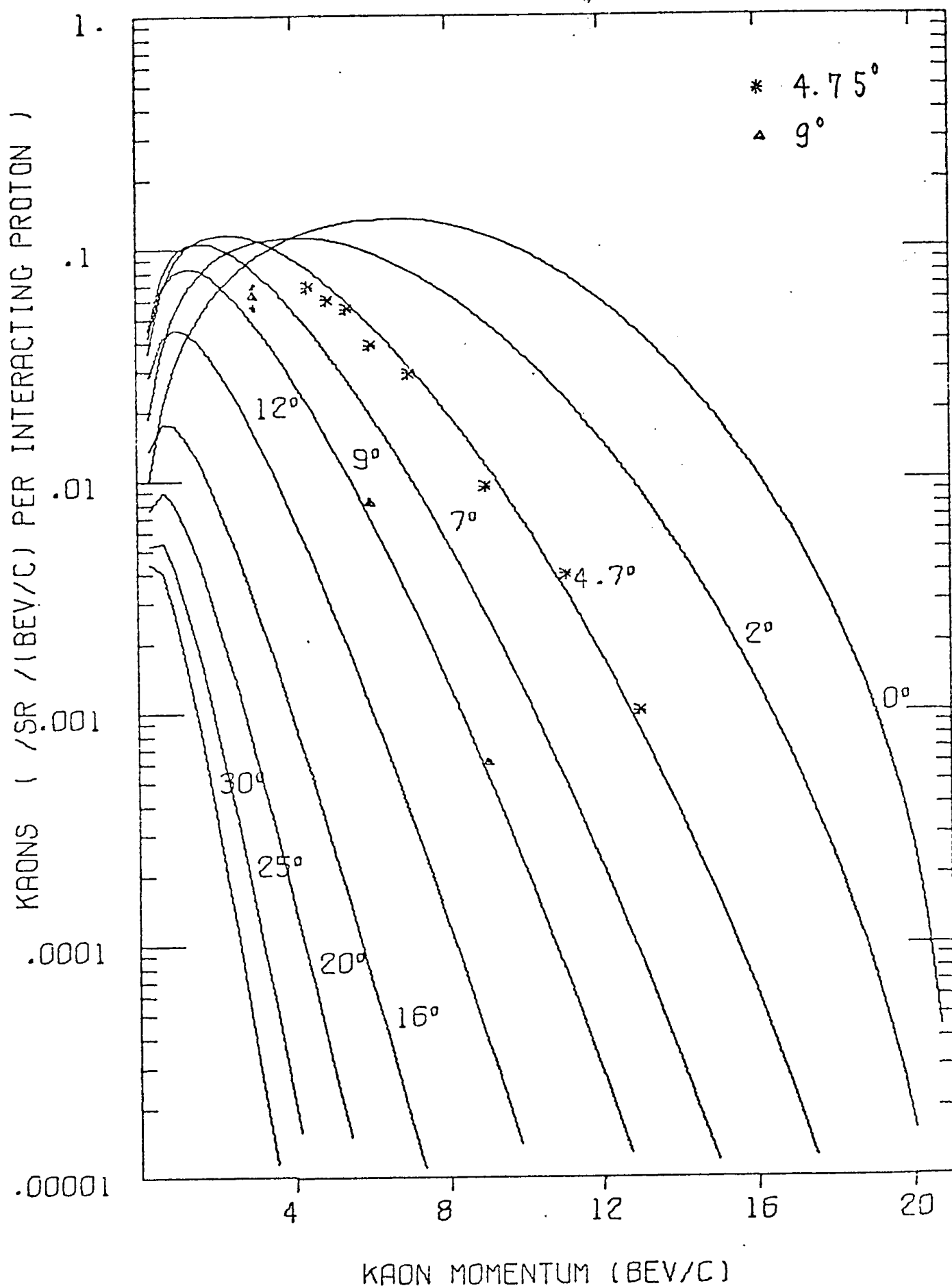
23.1 BEV/C   P-BE.   POSITIVE KAON PRODUCTION
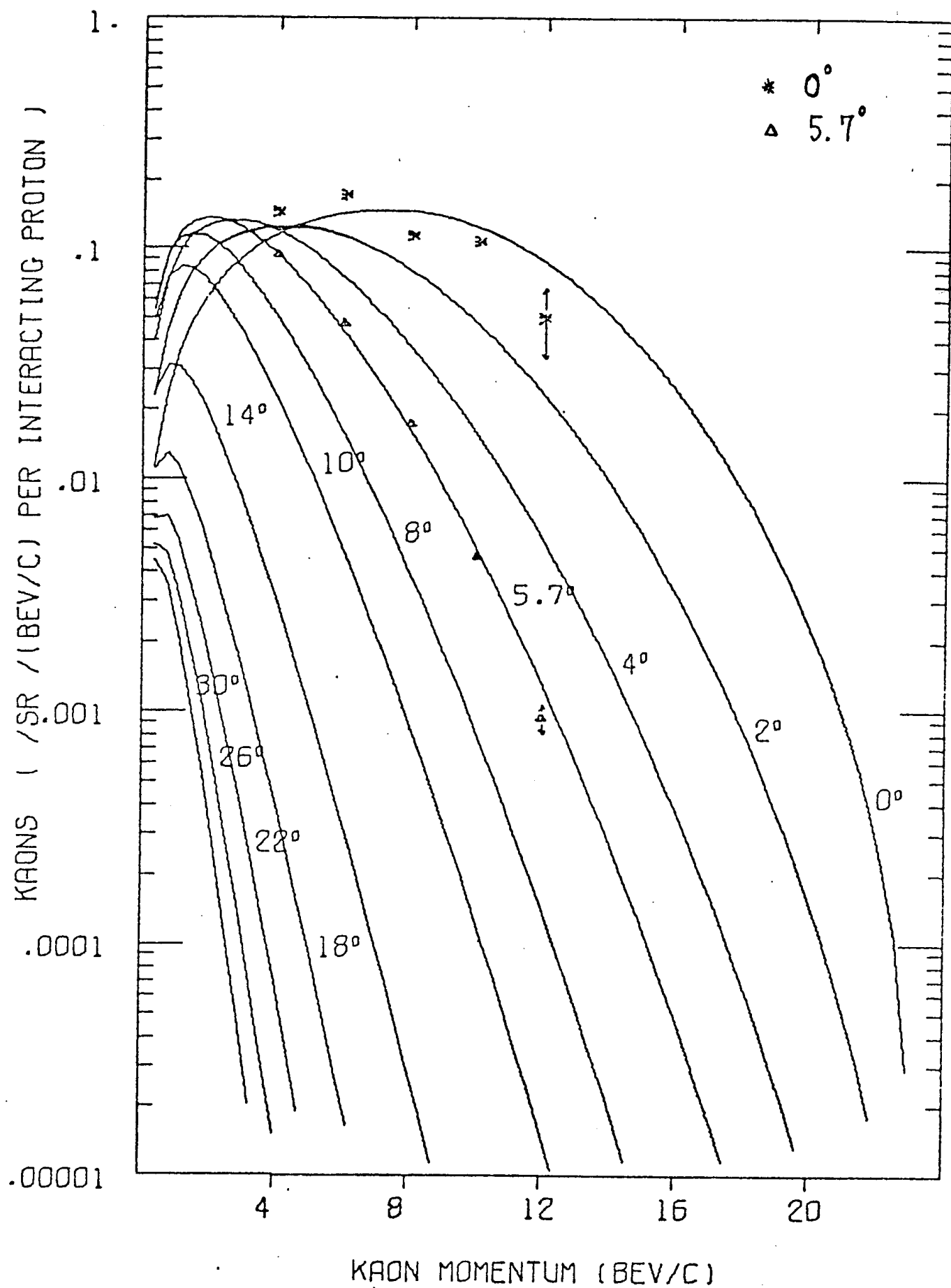
Figure 5

27.0 BEV/C   P-BE.   POSITIVE KAON PRODUCTION
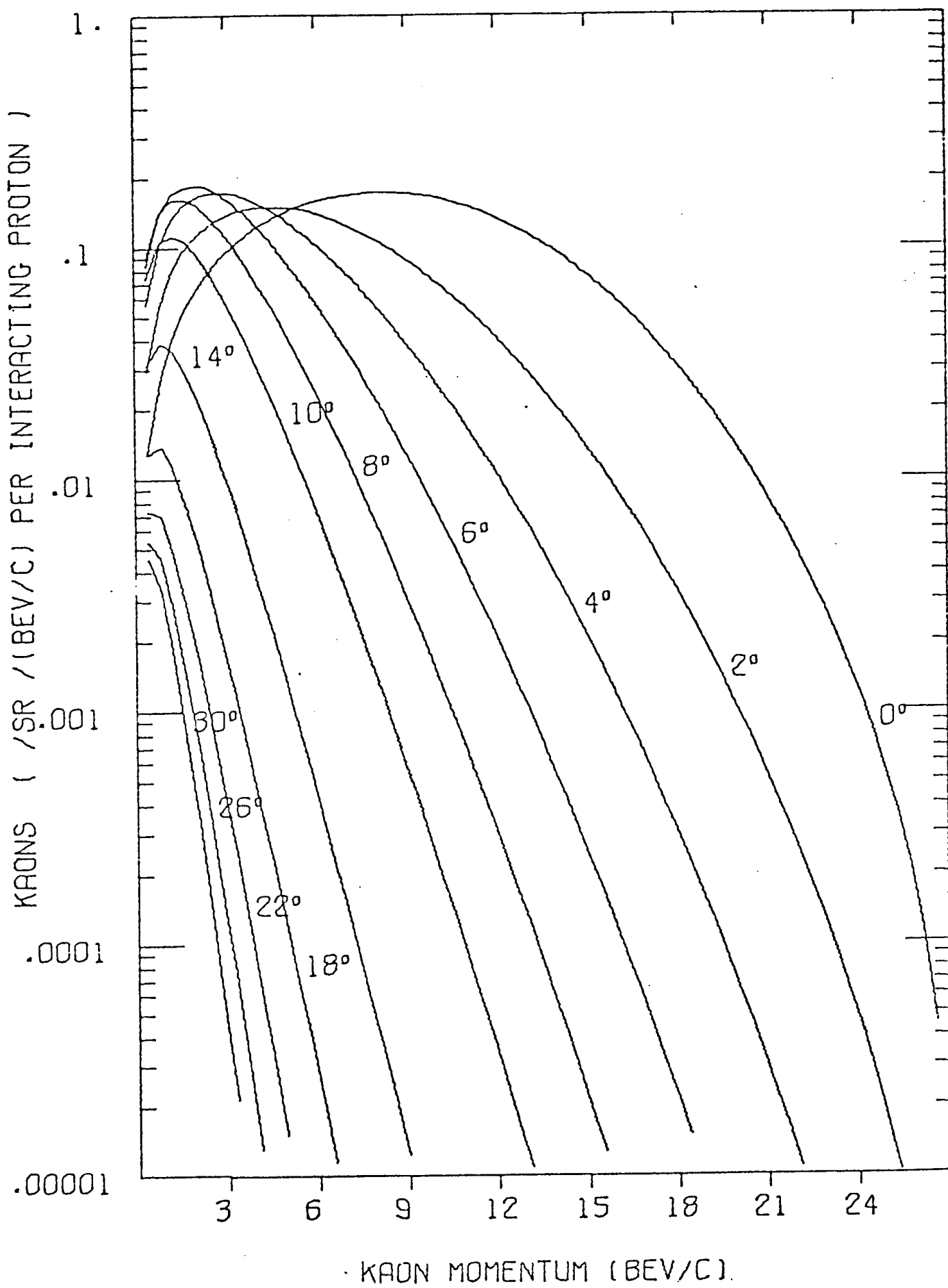
Figure 6

30.9 BEV/C   P-BE.   POSITIVE KAON PRODUCTION
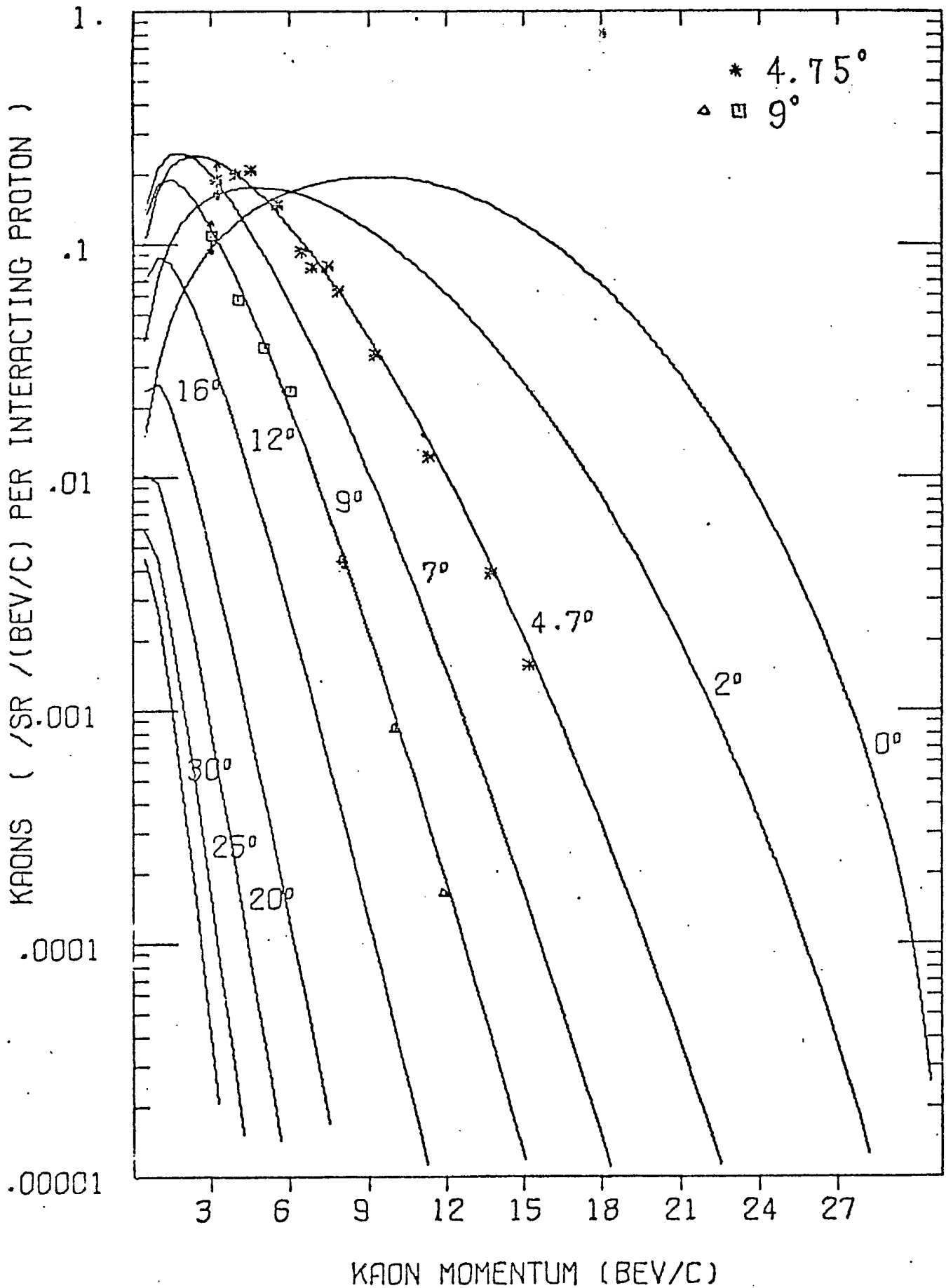
Figure 7

33.9 BEV/C   P-BE.   POSITIVE KAON PRODUCTION
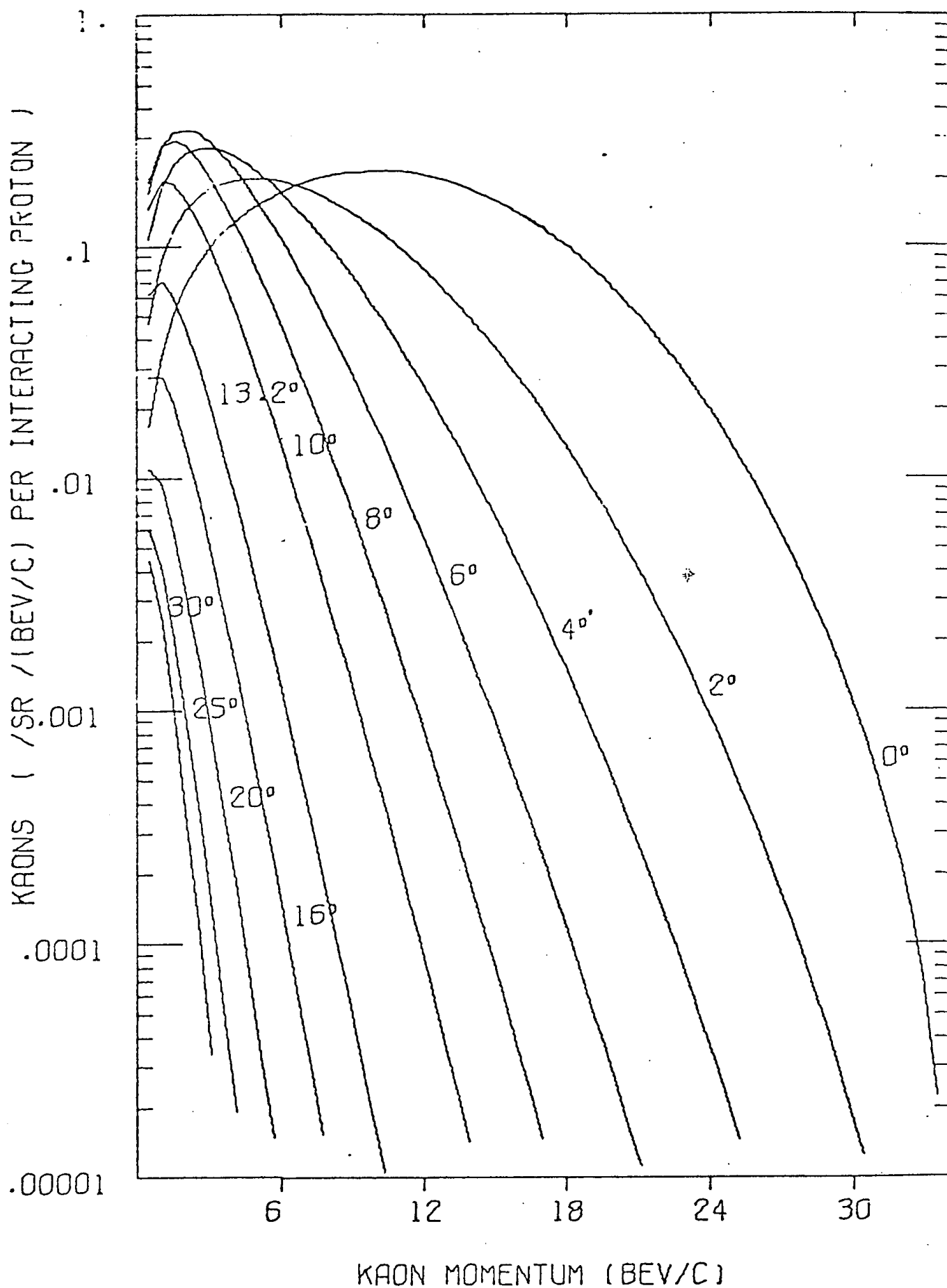
Figure 8

10.9 BEV/C P-BE. NEGATIVE KAON PRODUCTION

KAON MOMENTUM (BEV/C)
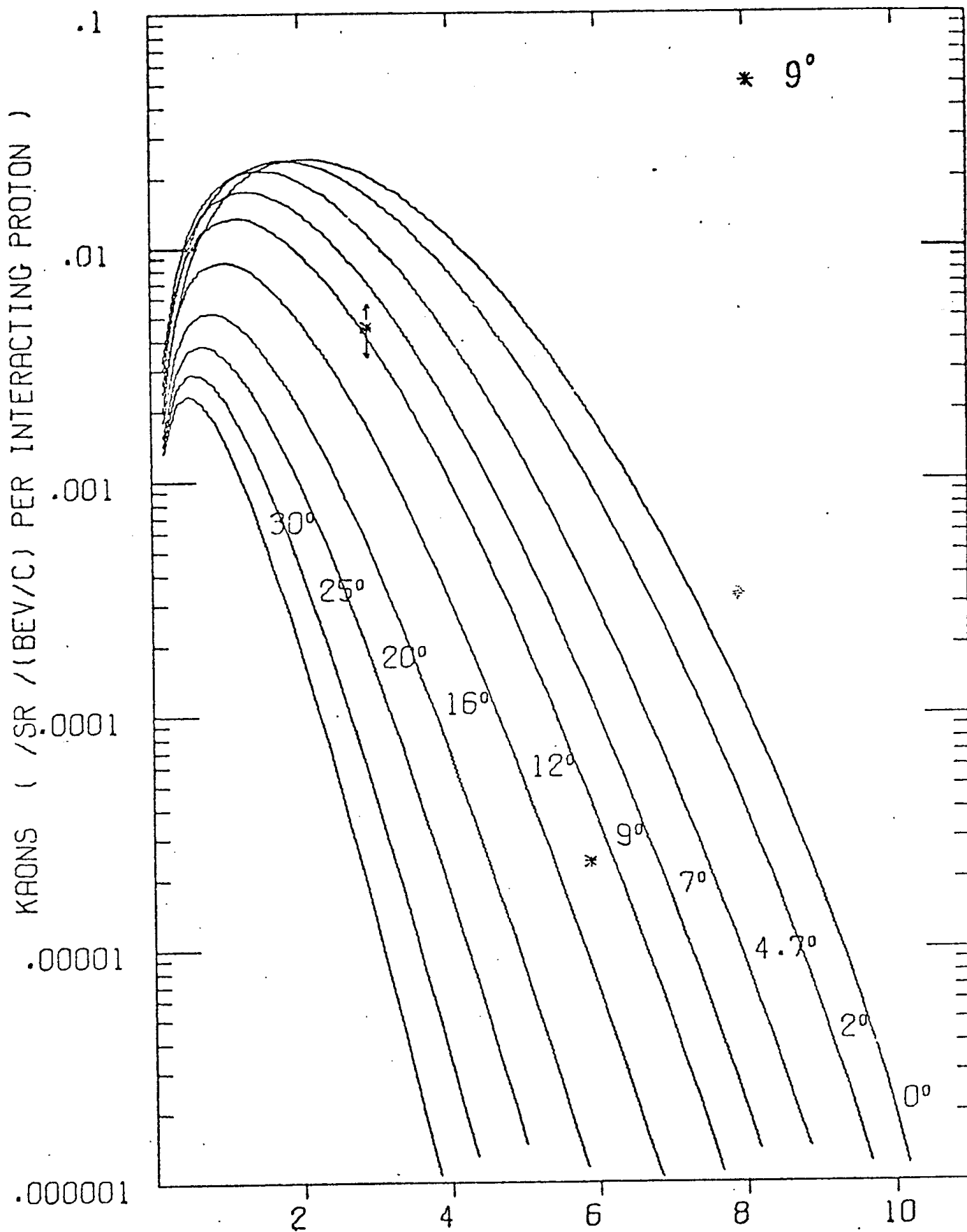
Figure 9

13.4 BEV/C   P-BE.   NEGATIVE KAON PRODUCTION
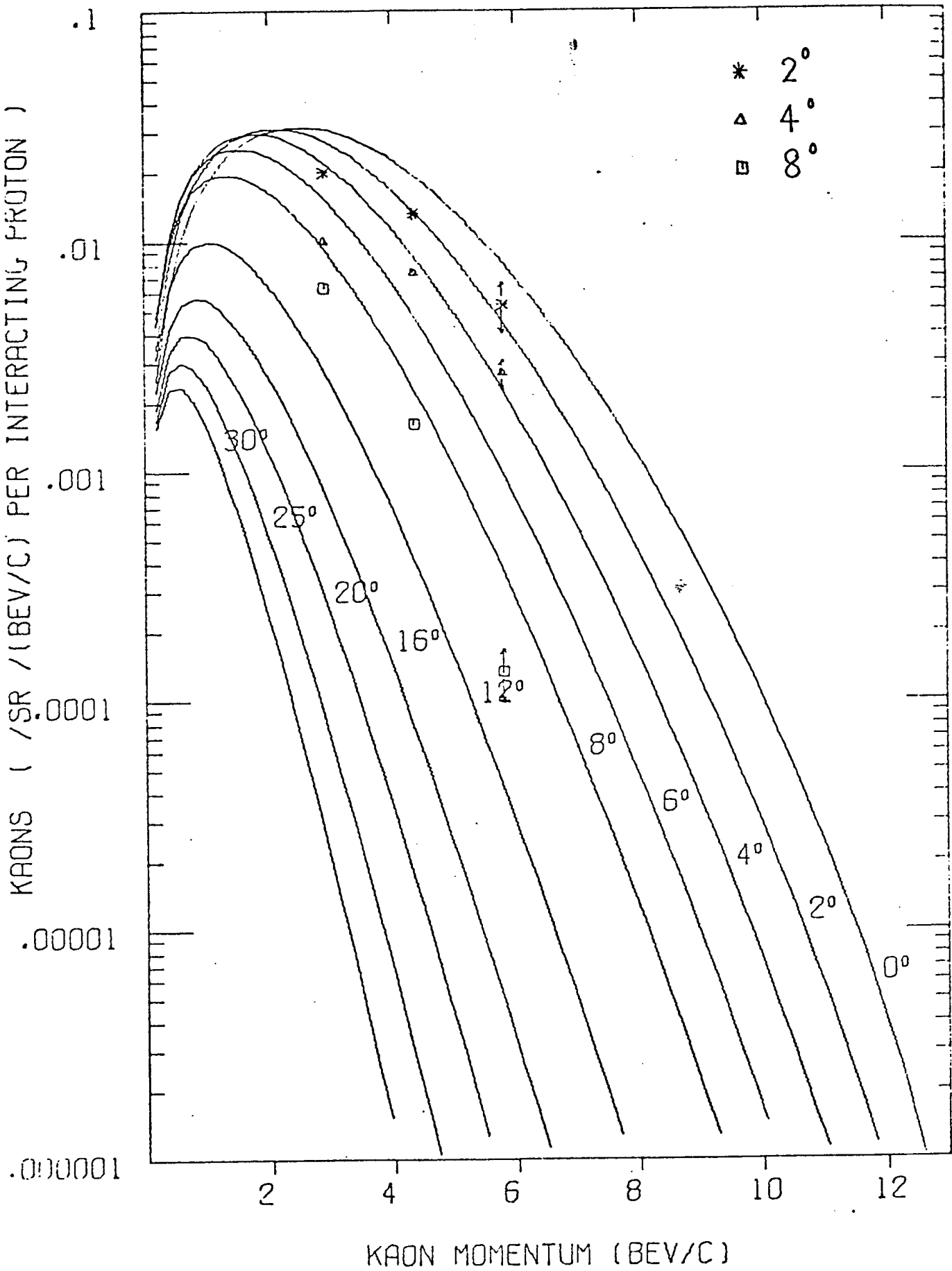
Figure 10
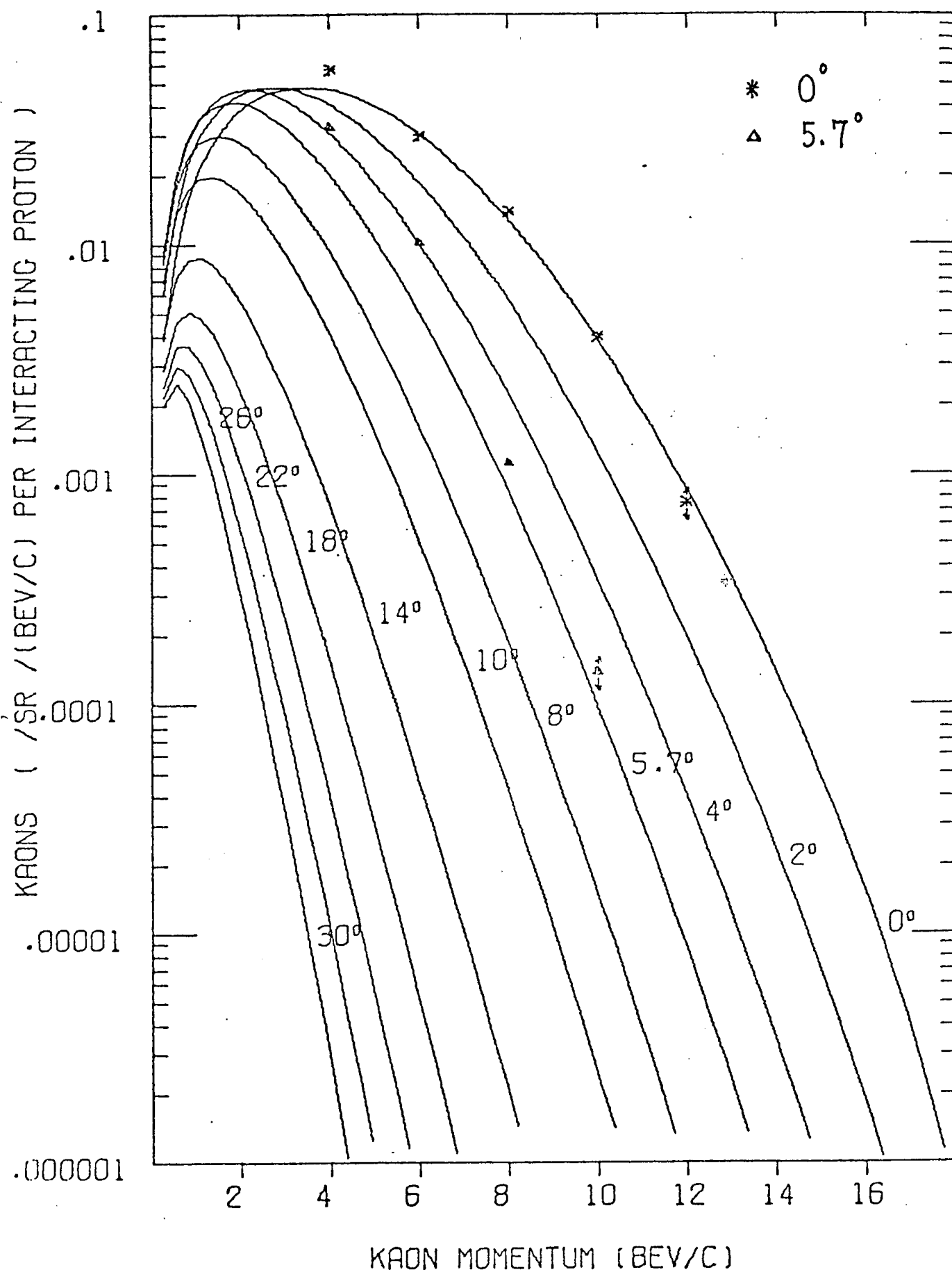
Figure 11

20.9 BEV/C   P-BE.   NEGATIVE KAON PRODUCTION
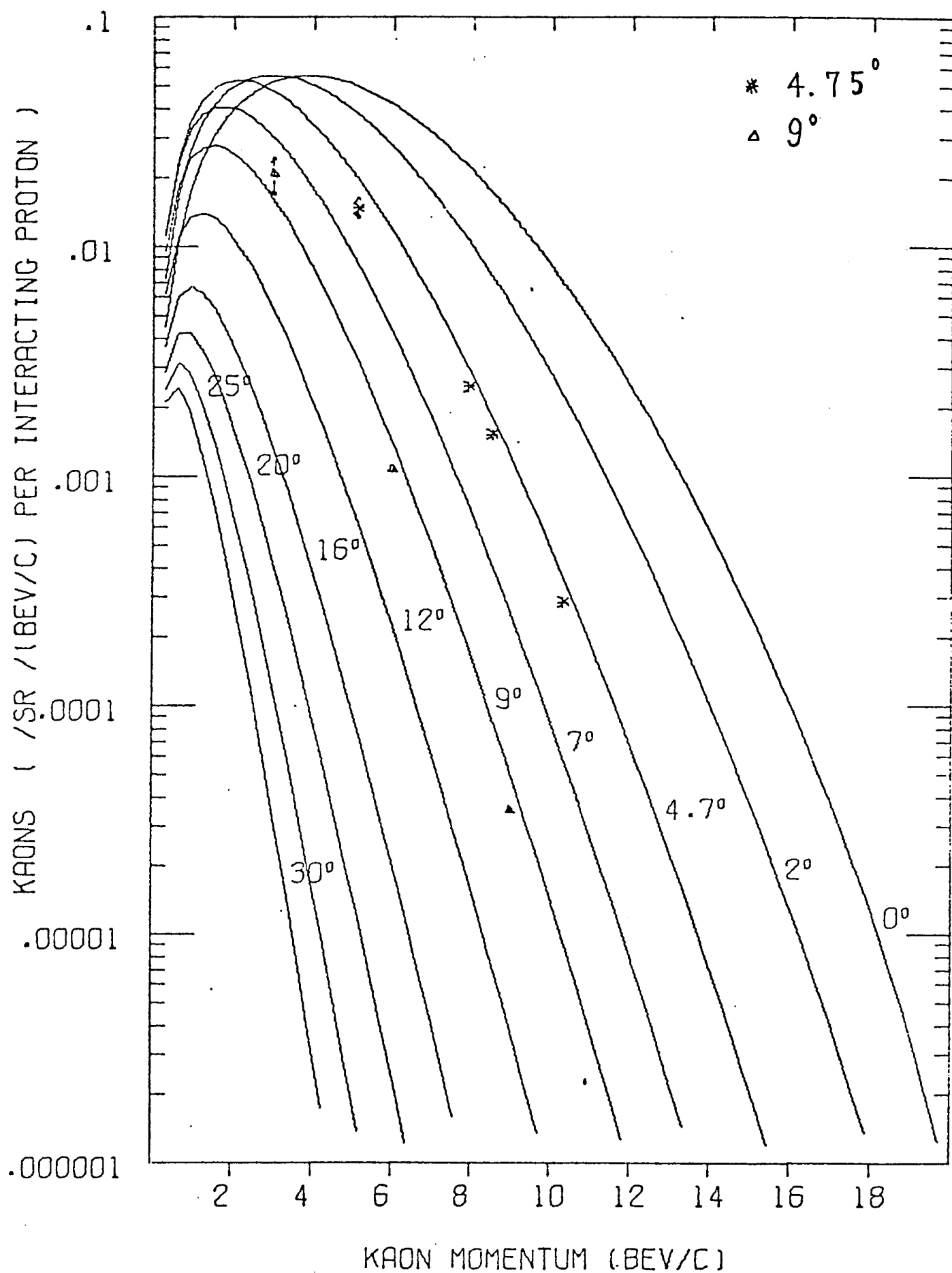
Figure 12

23.1 BEV/C   P-BE.   NEGATIVE KAON PRODUCTION
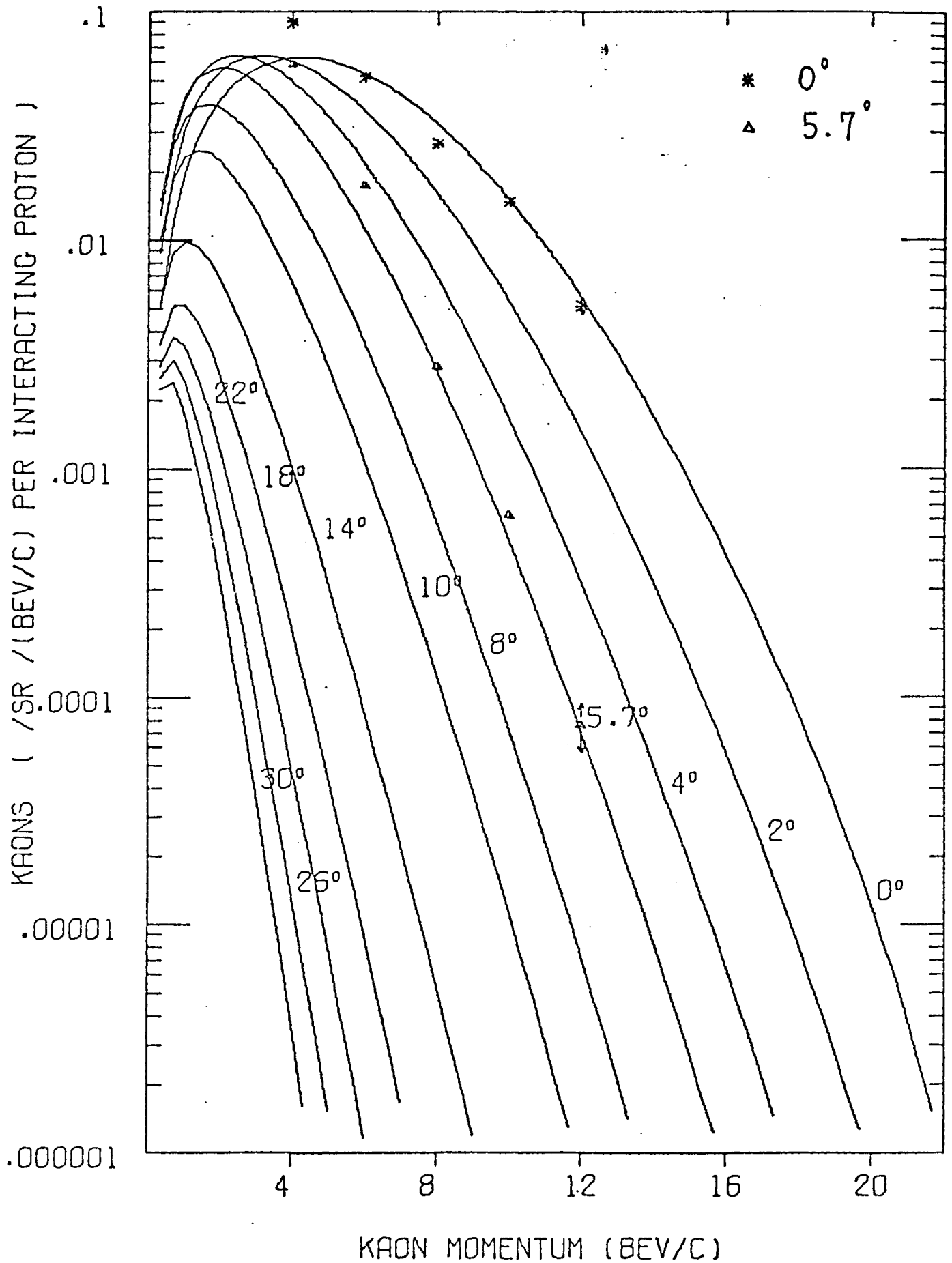
Figure 13

27.0 BEV/C   P-BE.. NEGATIVE KAON PRODUCTION
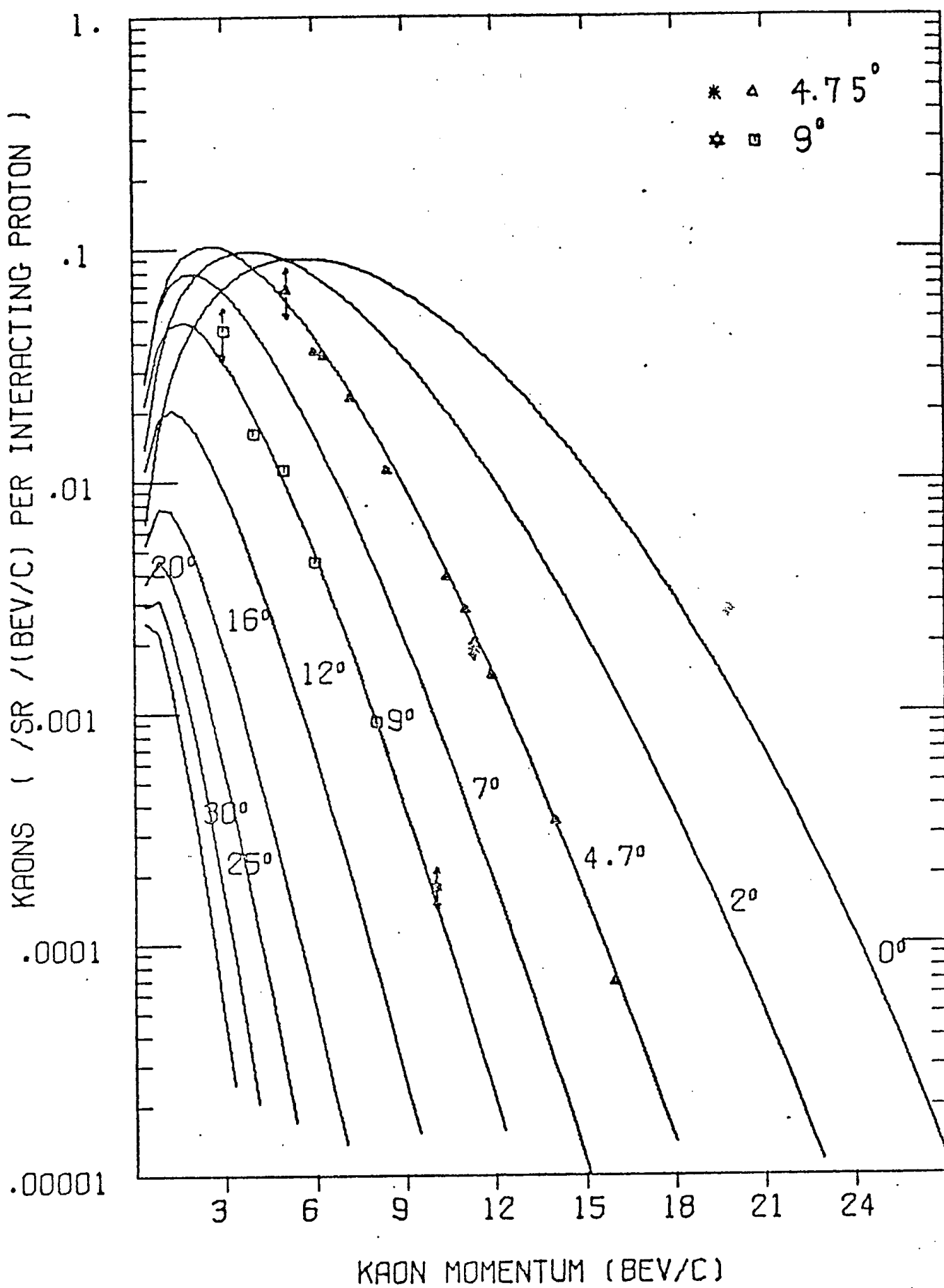
Figure 14

Figure 15

33.9 BEV/C   P-BE.   NEGATIVE KAON PRODUCTION
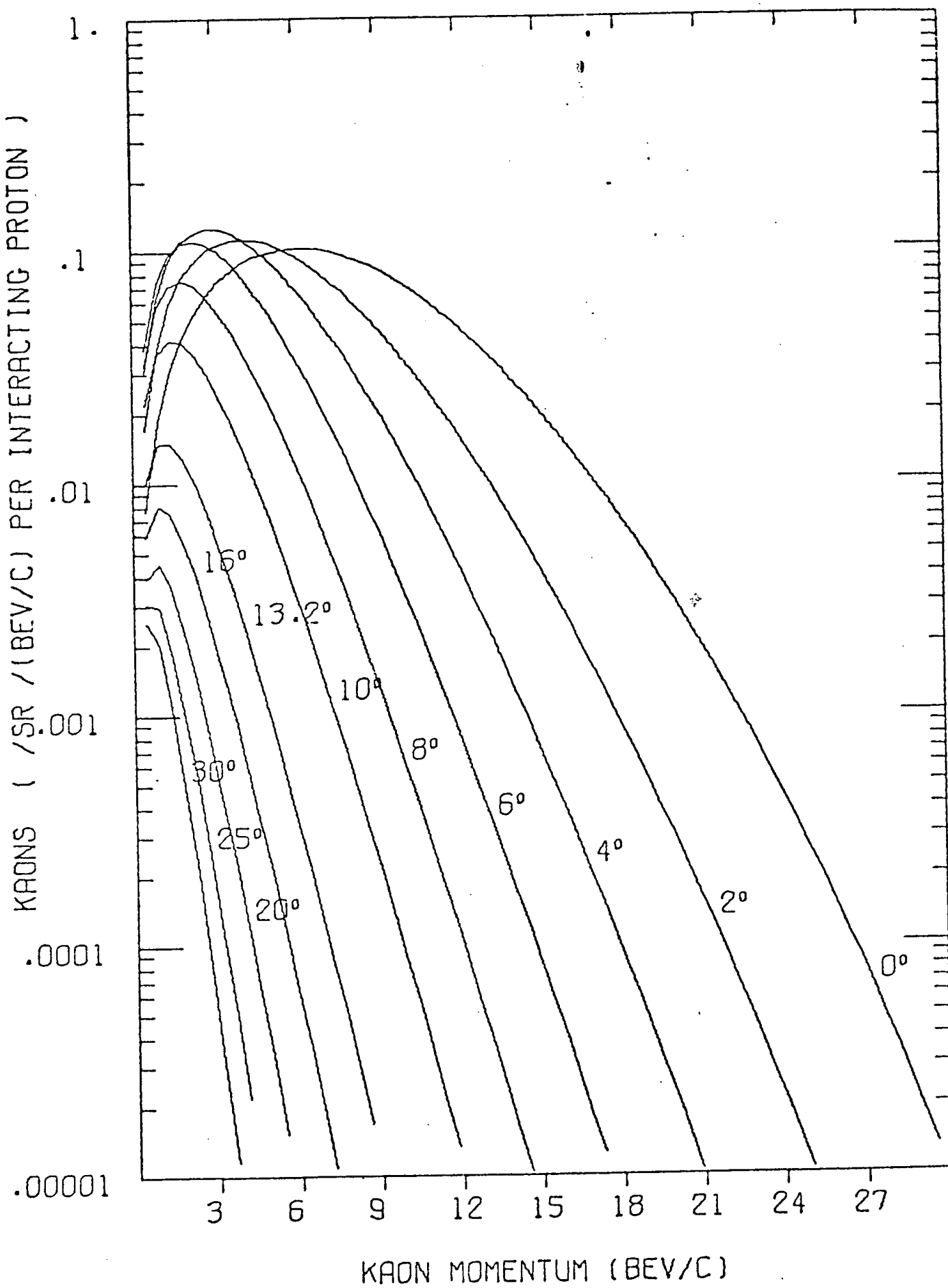
Figure 16

10.9 BEV/C   P-BE.   ANTIPROTON PRODUCTION
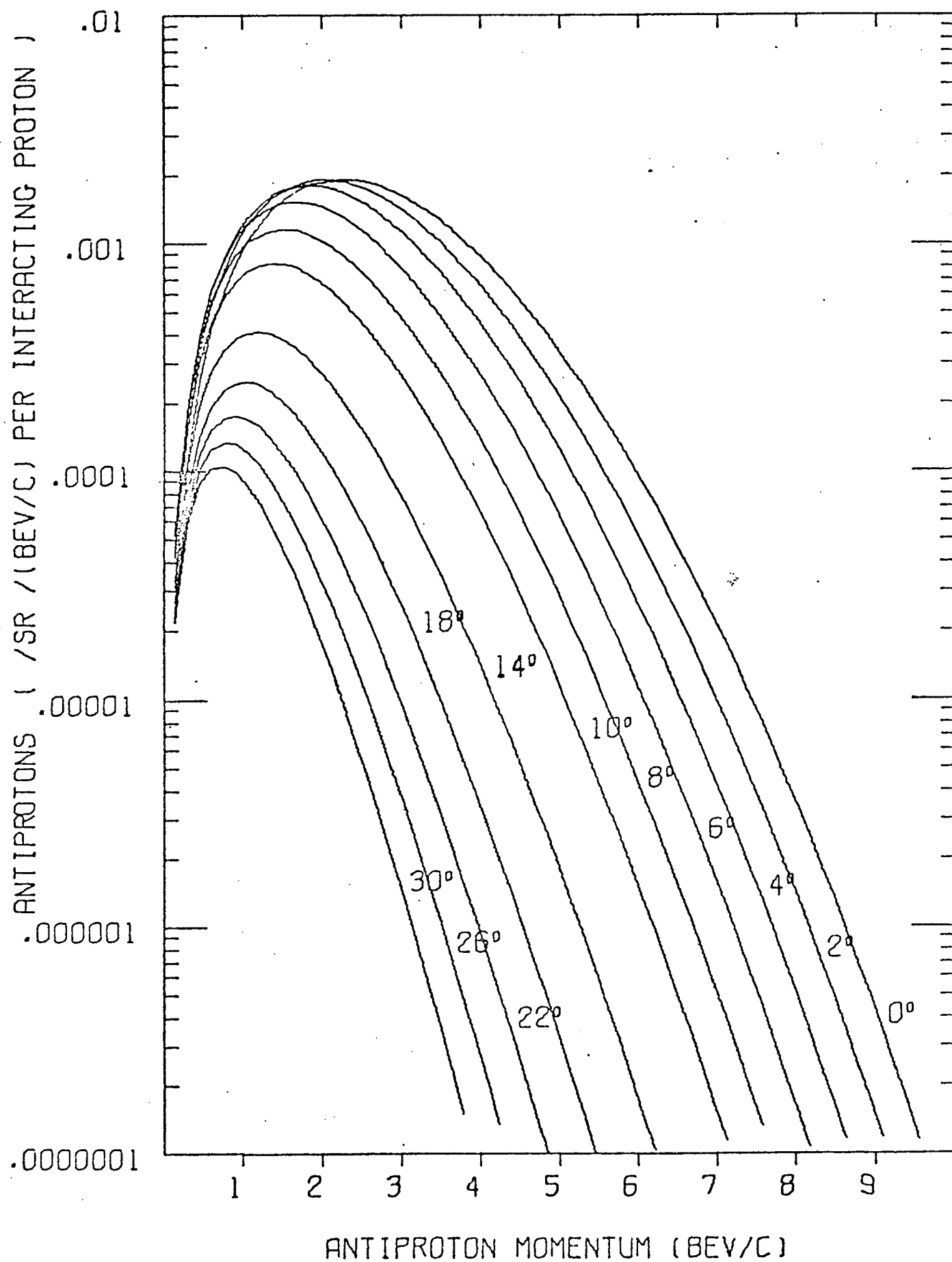
Figure 17

13.4 BEV/C   P-BE.   ANTIPROTON PRODUCTION
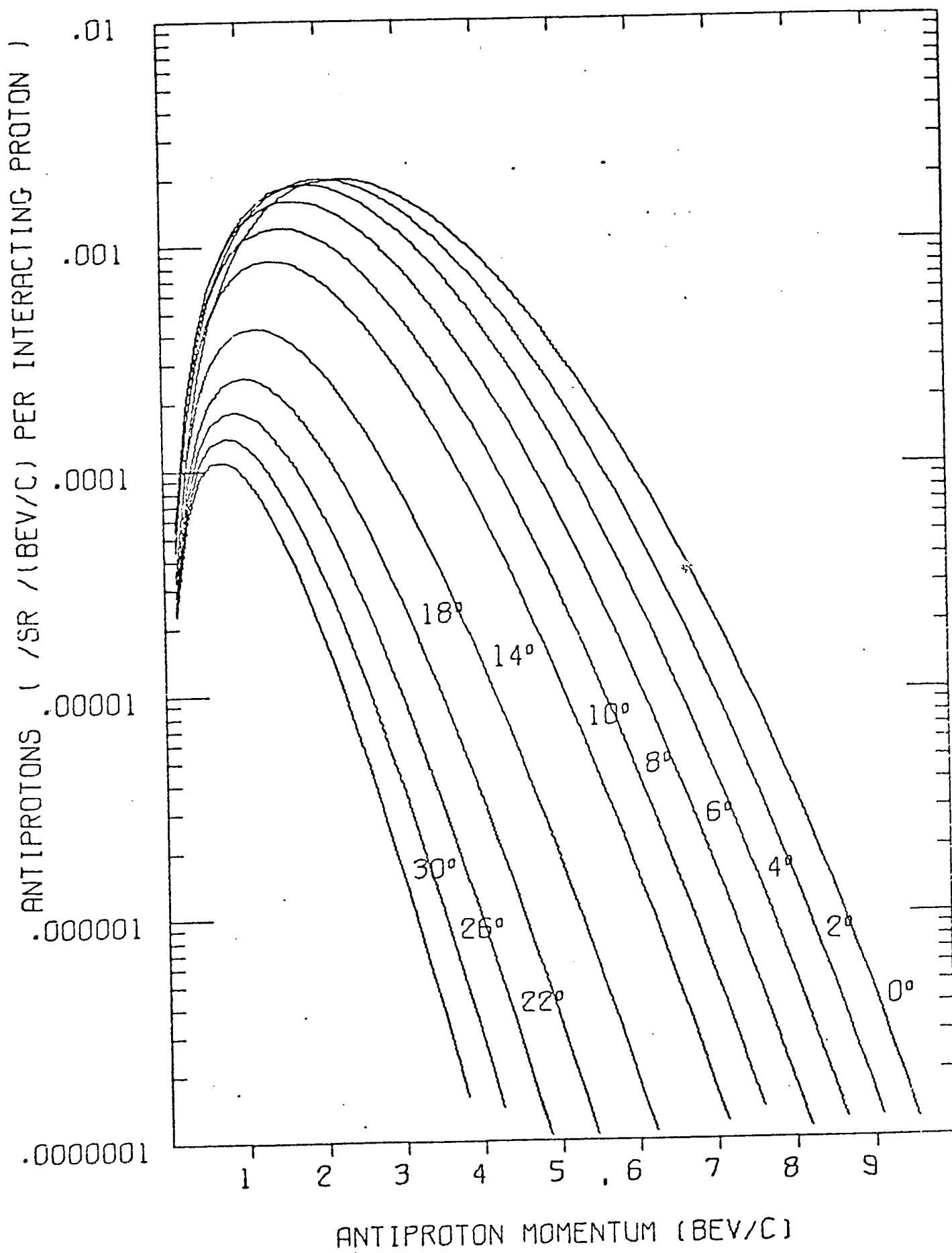
Figure 18

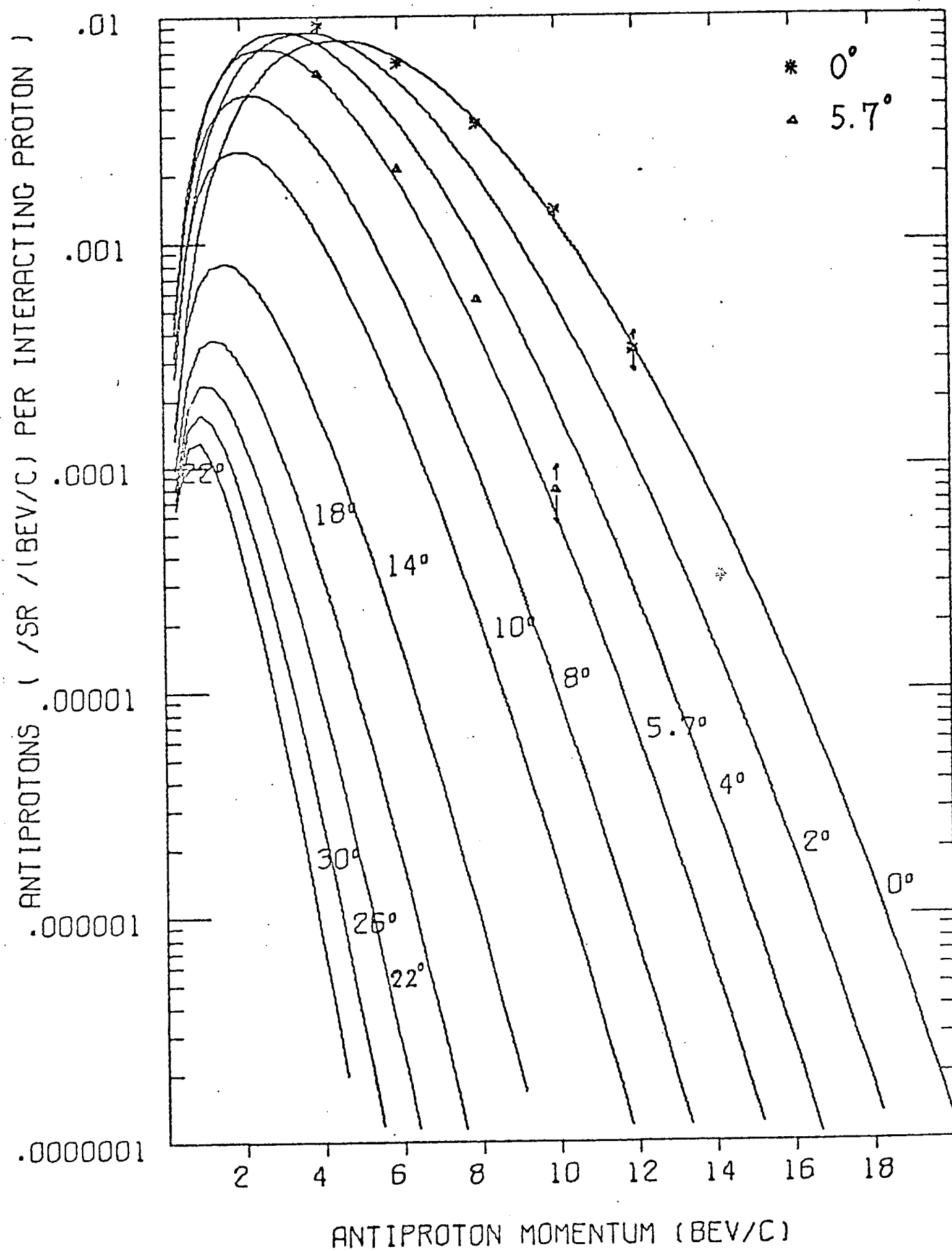18.8 BEV/C   P-BE.   ANTIPROTON PRODUCTION
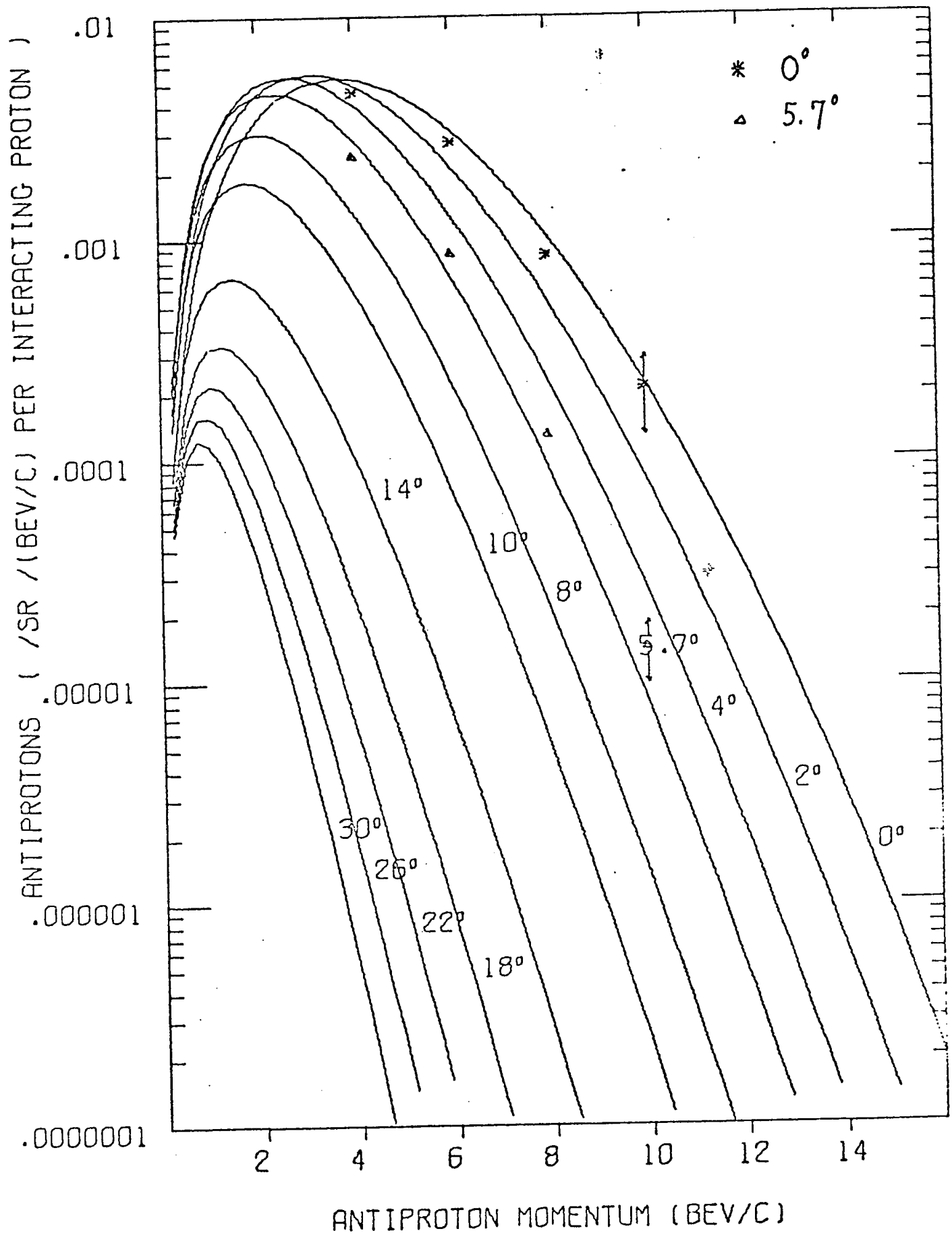
Figure 19

20.9 BEV/C P-BE. ANTIPROTON PRODUCTION
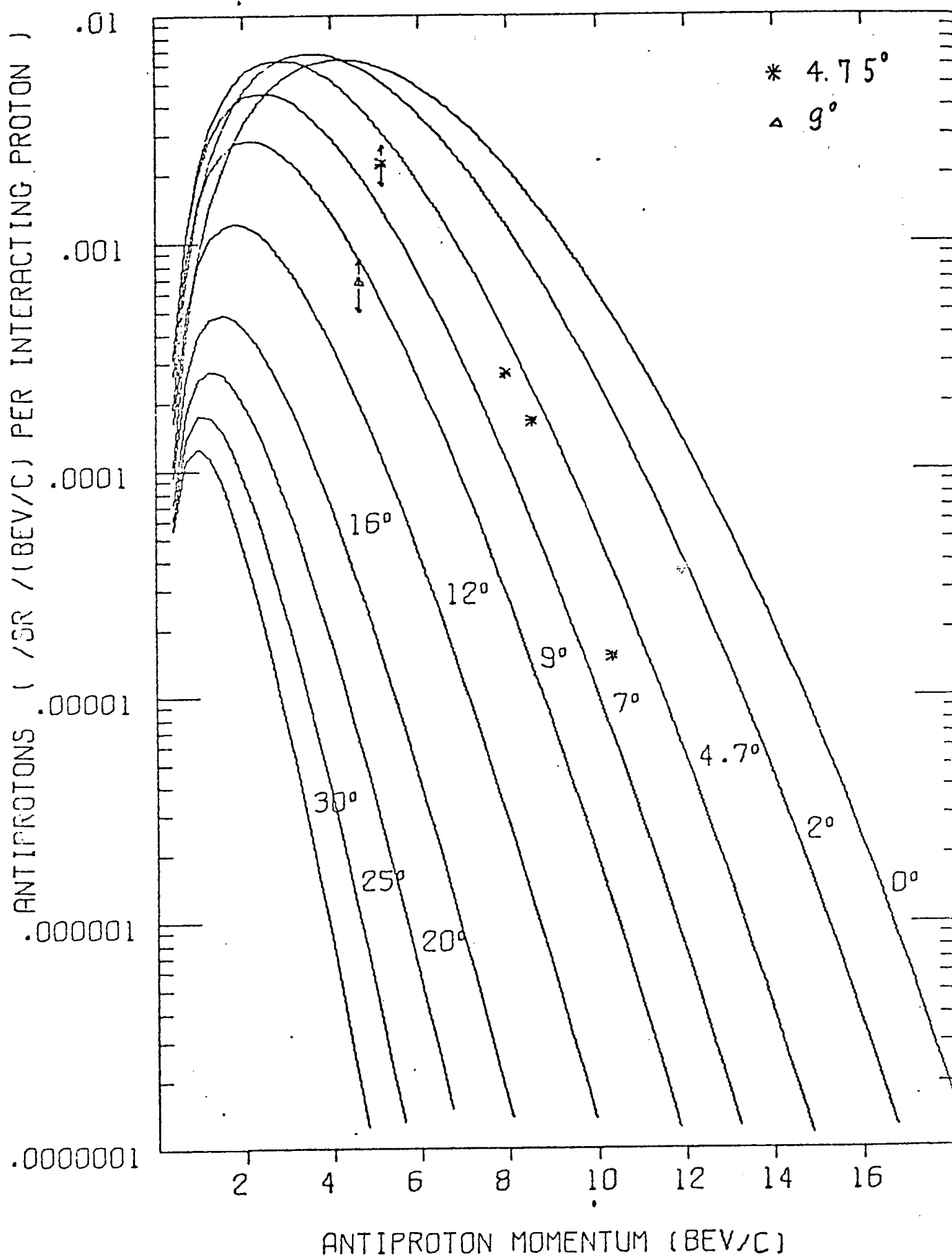
Figure 20

23.1 BEV/C   P-BE.   ANTIPROTON PRODUCTION

Figure 21

25.9 BEV/C   P-BE.   ANTIPROTON PRODUCTION
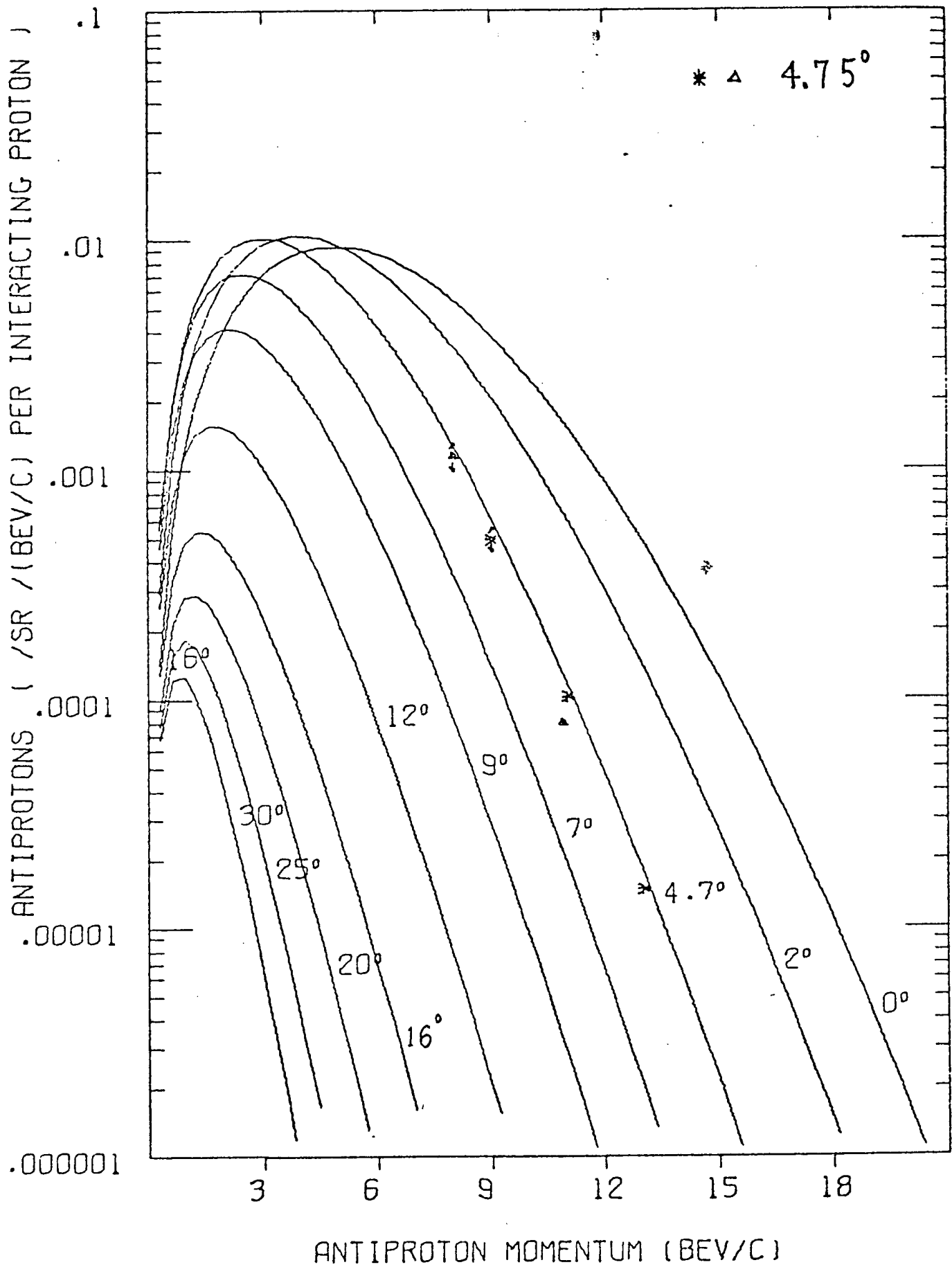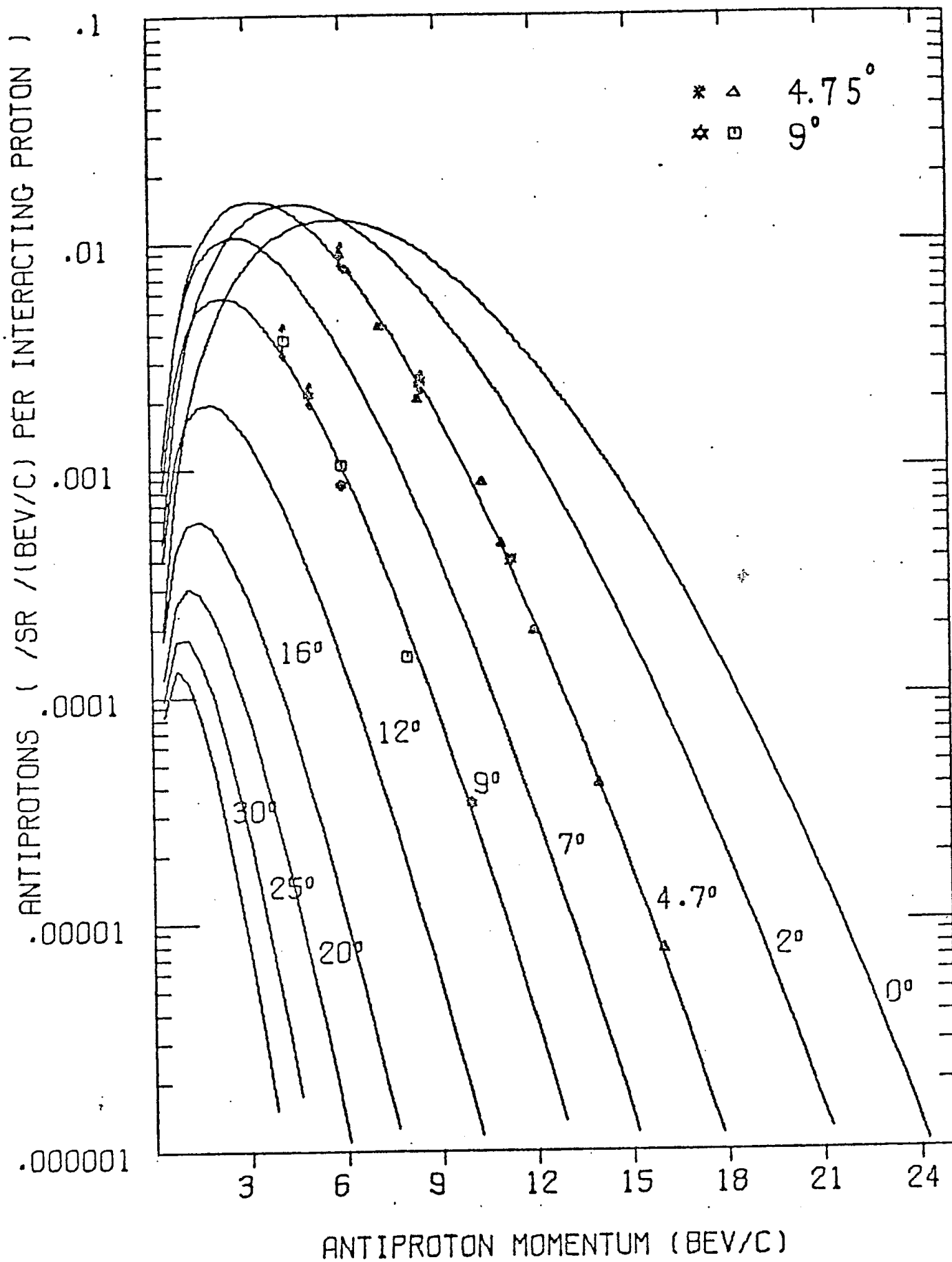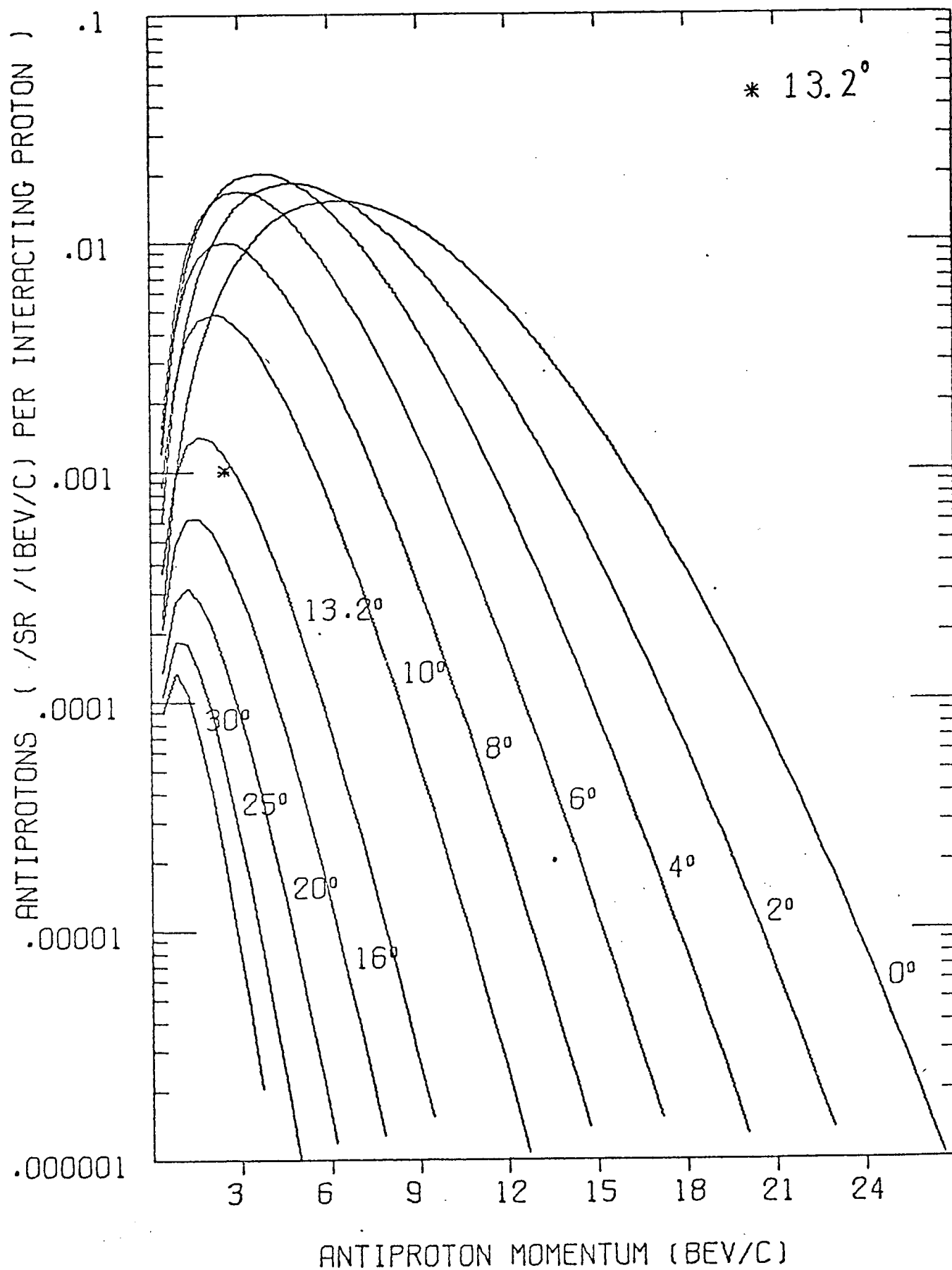
Figure 22

Figure 23

Figure 24